

Supplementary Material (ESI) for Lab on a Chip

Selective Adsorption of Unmethylated DNA on ZnO Nanowires for Separation of Methylated DNA

Marina Musa,^{*‡a} Zetao Zhu,^{*b} Hiromi Takahashi,^a Wataru Shinoda,^c Yoshinobu Baba^{*ade}
and Takao Yasui^{*bd}

^aDepartment of Biomolecular Engineering, Graduate School of Engineering, Nagoya University, Furo-cho, Chikusa-ku, Nagoya 464-8603, Japan;

^bDepartment of Life Science and Technology, Tokyo Institute of Technology, Nagatsuta 4259, Midori-ku, Yokohama 226-8501, Japan

^cResearch Institute for Interdisciplinary Science, Okayama University, Okayama, 700-8530, Japan

^dInstitute of Nano-Life-Systems, Institutes of Innovation for Future Society, Nagoya University, Furo-cho, Chikusa-ku, Nagoya 464-8603, Japan.

^eInstitute of Quantum Life Science, National Institutes for Quantum Science and Technology (QST), Anagawa 4-9-1, Inage-ku, Chiba 263-8555, Japan.

*Correspondence to:

*M. Musa E-mail: marina-musa@g.ecc.u-tokyo.ac.jp;

*Z. Zhu Phone: +81-45-924-5520; E-mail: zhu.z.ag@m.titech.ac.jp;

*Y. Baba Phone: +81-52-789-4664; E-mail: babaymtt@chembio.nagoya-u.ac.jp;

*T. Yasui Phone: +81-45-924-5520; E-mail: yasuit@bio.titech.ac.jp.

‡Current address: Department of Chemistry, School of Science, The University of Tokyo, 7-3-1 Hongo, Bunkyo-ku, Tokyo 113-0033, Japan

Figure S1 Fabrication process of the microchannel mold and PDMS microchannel.

Figure S2 Fabrication process of the nanowire-based microfluidic device.

Figure S3 Characterization of the ZnO nanowires embedded in the microfluidic device.

Figure S4 Contact angles of the ZnO film and ZnO nanowires.

Figure S5 FTIR spectra of partially methylated DNAs with different methylation positions before and after being captured on ZnO nanowires.

Figure S6 Probability distribution of the unmethylated, methylated, and partially methylated DNAs with different methylation positions expressed against the distance from the ZnO surface.

Figure S7 Profile map of capture efficiencies of unmethylated, methylated, and partially methylated DNAs with different methylation levels and positions obtained using ZnO nanowire-based devices.

Figure S8 Capture efficiencies of ssDNA and dsDNA with different methylation levels.

Figure S9 Capture efficiencies of the involved polynucleotides, PolyA, PolyT, PolyC, and PolyG.

Table S1 Zeta potentials of the DNA, ZnO nanowires, and ZnO nanowires covered by a ZnO layer.

Table S2 Peak positions extracted from FTIR spectra.

Table S3 Oligonucleotide sequences used in this study.

Table S4 Comparison table of microfluidic MeDIP-seq and our method.

Movie S1 The adsorption process of unmethylated DNA (CCCCC) on ZnO surface (MD simulation), related to Figure 2

Movie S2 The adsorption process of methylated DNA (CmCmCmCmCm) on ZnO surface (MD simulation), related to Figure 2

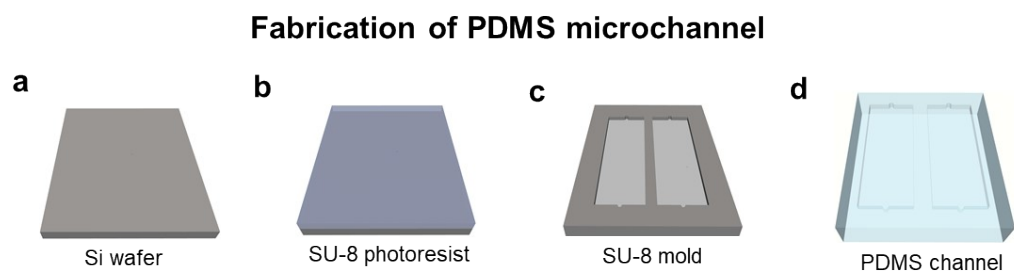


Figure. S1. Fabrication process of the microchannel mold and PDMS microchannel.

Fabrication of oxide nanowire microfluidic device

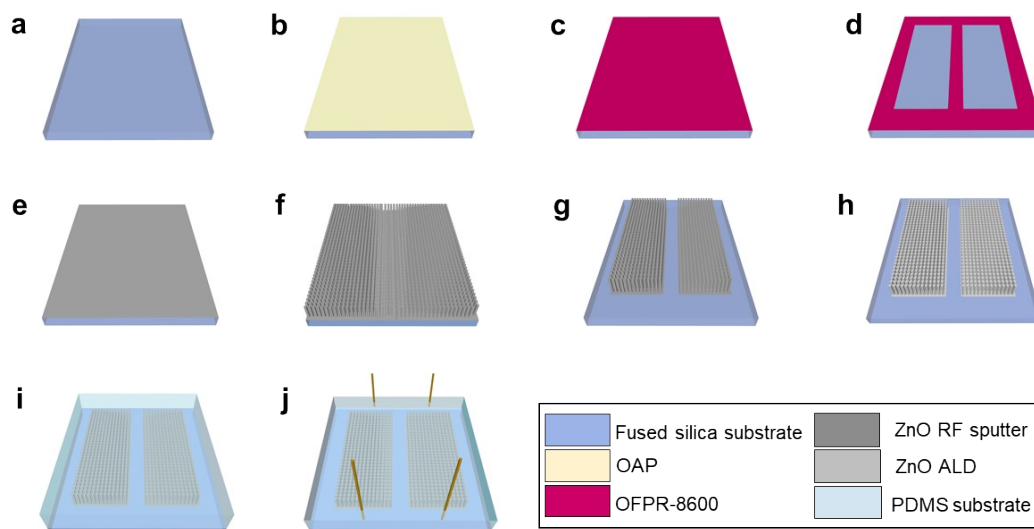


Figure. S2. Fabrication process of the nanowire-based microfluidic device.

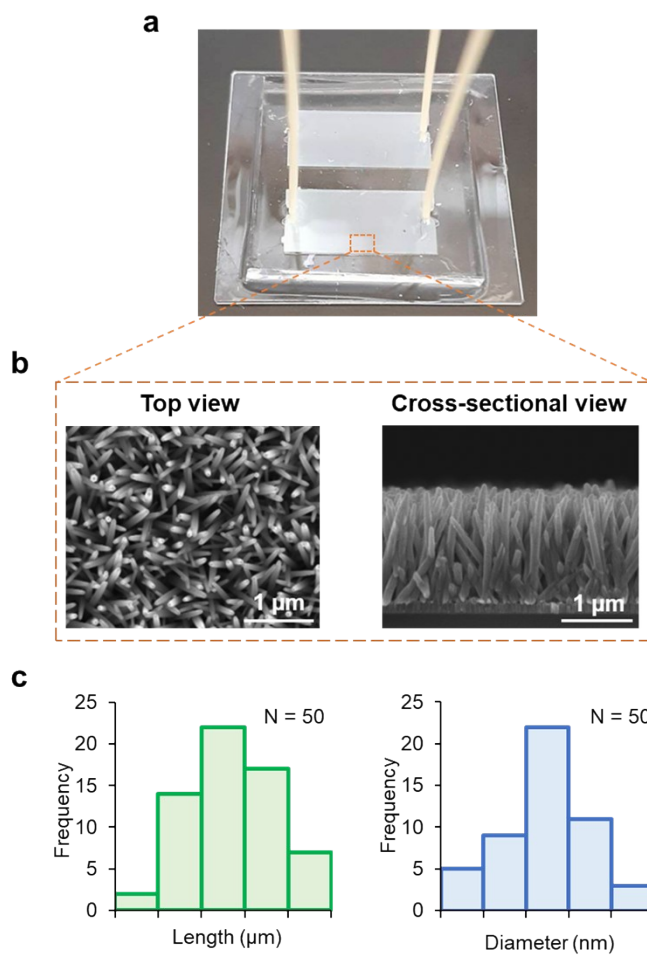


Figure. S3. Characterization of the ZnO nanowires embedded in the microfluidic device. (a) Image of the microfluidic device. (b) Top and cross-sectional views of ZnO nanowires embedded in the device. (c) Frequency distributions of the length and diameter of the nanowires.

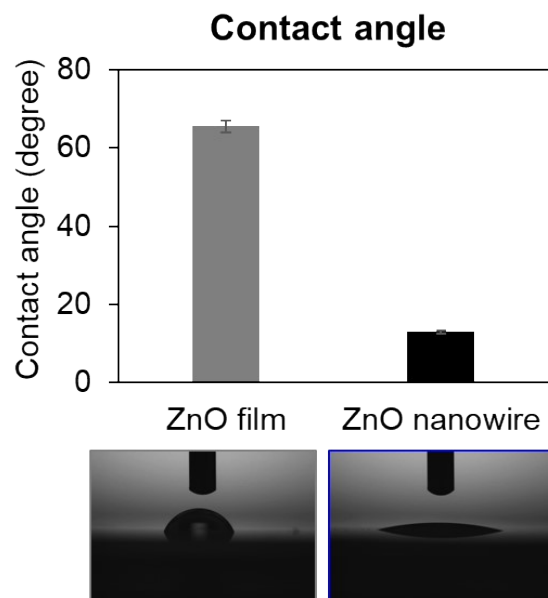


Figure. S4. Contact angles of the ZnO film and ZnO nanowires.

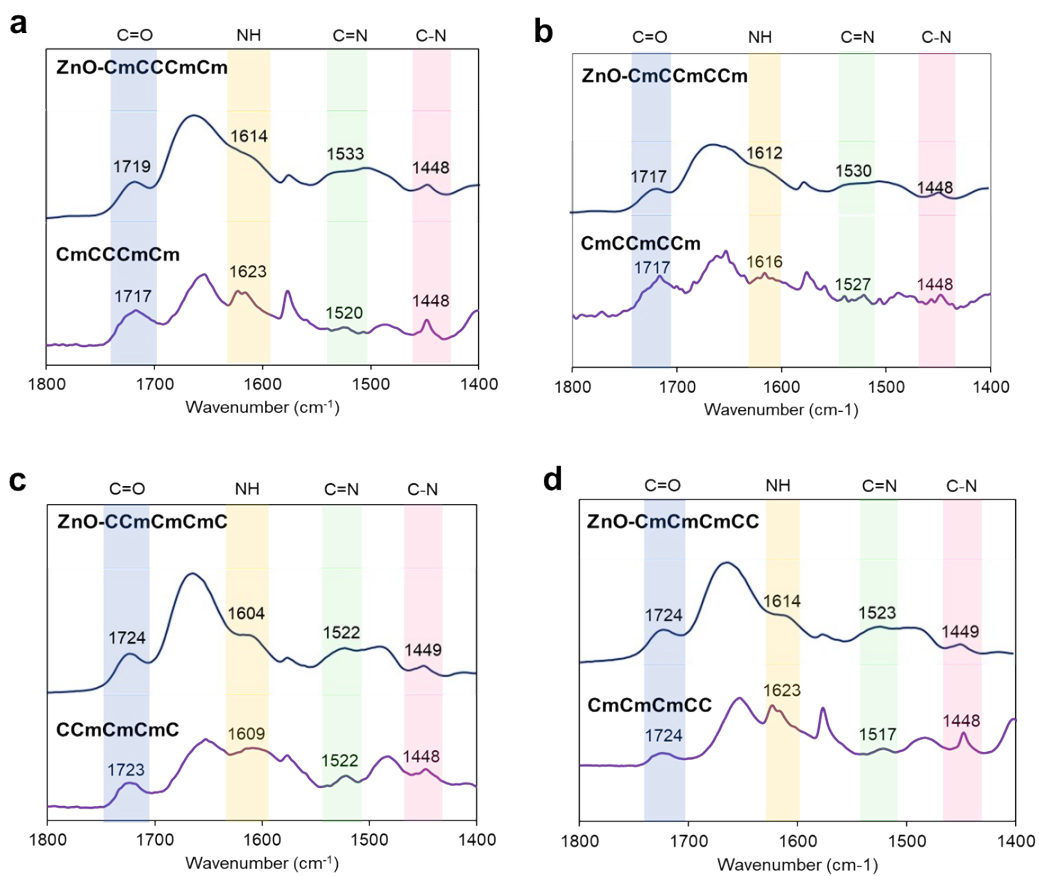


Figure. S5. FTIR spectra of partially methylated DNAs with different methylation positions before and after being captured on ZnO nanowires. (a) CmCCCmCm and ZnO-CmCCCmCm. (b) CmCCmCCm and ZnO-CmCCmCCm. (c) CCmCmCmC and ZnO-CCmCmCmC. (d) CmCmCmCC and ZnO-CmCmCmCC.

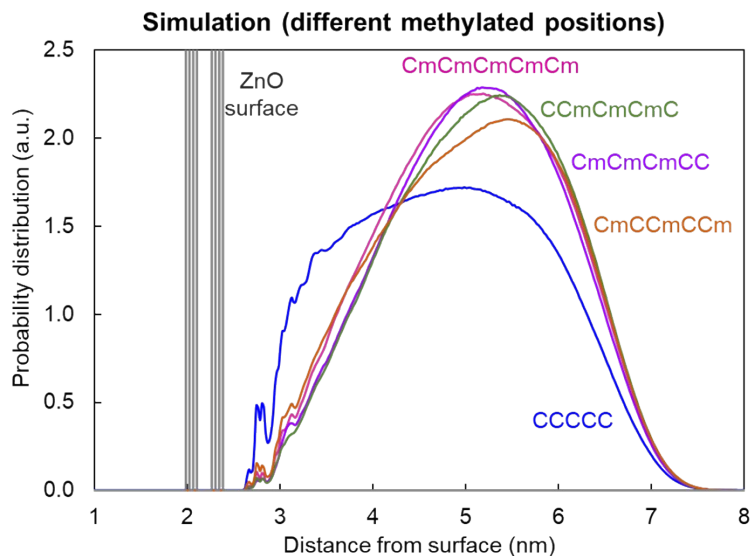


Figure. S6. Probability distributions of the unmethylated, methylated, and partially methylated DNAs with different methylation positions expressed against the distance from the ZnO surface. A higher probability distribution peak of unmethylated DNAs on adjacent regions of the ZnO surface was observed than the peaks of partially and fully methylated DNAs. Compared to the sharp peak in the distributions of unmethylated and fully methylated DNAs, the partially methylated DNAs exhibited a peak on the further regions of the ZnO surface, similar to the distribution peak of the fully methylated DNAs.

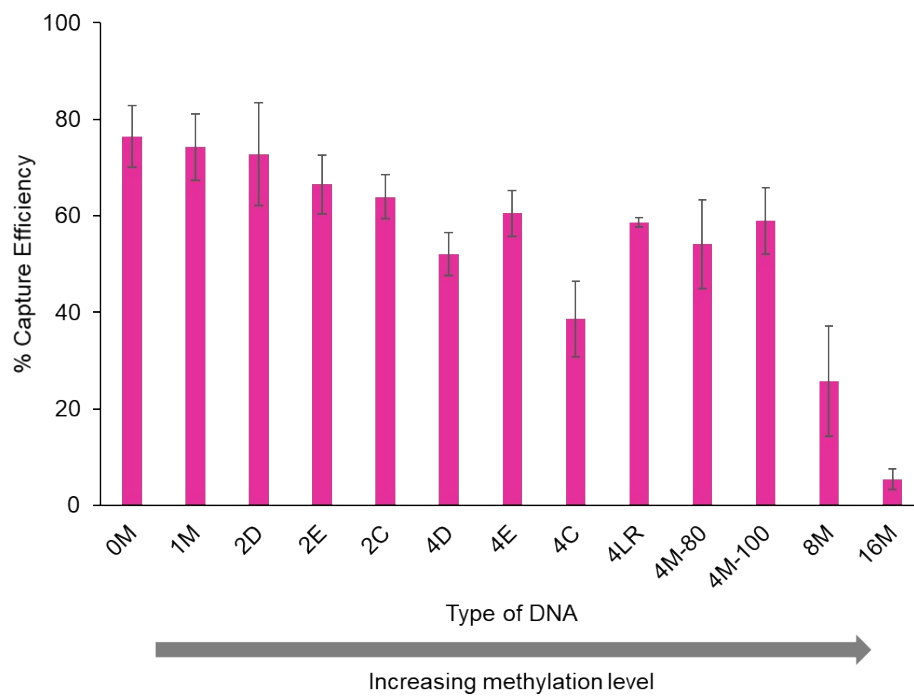


Figure. S7. Profile map of capture efficiencies of unmethylated, methylated, and partially methylated DNAs with different methylation levels and positions obtained using ZnO nanowire-based device.

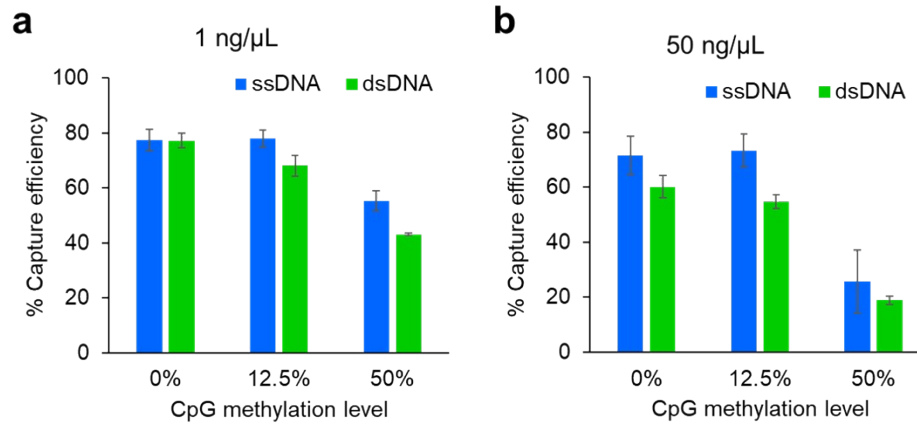


Figure. S8. Type or paste legend here. Capture efficiencies of ssDNA and dsDNA with different methylation levels. (a) Low concentration: 1 ng/μL. (b) High concentration: 50 ng/μL. The influence of DNA chain structure, whether it was single or double-stranded, on capture efficiency was investigated. The results showed that the capture efficiency of dsDNA was inferior to that of ssDNA.

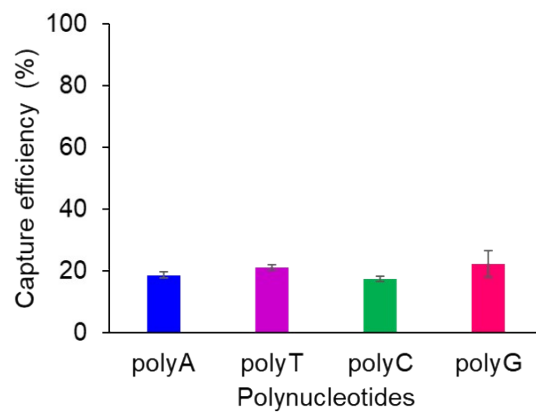


Figure. S9. Capture efficiencies of the involved polynucleotides, polyA, polyT, polyC, and polyG. Capture efficiencies of polynucleotides associated with polyA, polyT, polyC, and polyG were analyzed to validate the influence of polynucleotide composition on capture efficiency.

Table S1. Zeta potentials of the DNA, ZnO nanowires, and ZnO nanowires covered by an ALD ZnO layer.

Substances	Zeta potential (mV)
DNA	-50.8
ZnO nanowire	8.54
ZnO/ZnO nanowire (after ALD)	23.78

The zeta potential increased from 8.54 mV to 23.78 mV after ALD of the ZnO layer, which facilitates its adsorption capability for the negatively charged DNA.

Table S2. Peak positions extracted from FTIR spectra of unmethylated, methylated, and partially methylated DNAs with different methylation positions before and after being captured on ZnO nanowires.

Functional groups	FTIR wavenumber (cm ⁻¹)			
	C=O	N-H	C=N	C-N
CCCCC	1718	1624	1540	1448
ZnO-CCCCC	1724	1617	1528	1417
CmCmCmCmCm	1718	1623	1521	1448
ZnO-CmCmCmCmCm	1717	1617	1521	1448
CmCmCmCC	1724	1623	1517	1448
ZnO-CmCmCmCC	1724	1614	1523	1449
CmCCCmCm	1717	1623	1520	1448
ZnO-CmCCCmCm	1719	1614	1533	1448
CmCCmCCm	1717	1616	1527	1448
ZnO-CmCCmCCm	1717	1612	1530	1448
CCmCmCmC	1723	1609	1522	1448
Poly-CCmCmCmC	1724	1604	1522	1449

Table S3. Oligonucleotide sequences used in this study.

Oligonucleotides	Sequence (5' – 3')
0% CpG methylation (0M)	ATACGCGTACTGCGGTTCGCGATCGCGCTCTCGCGC TGACGGTTCGTCGCGCGTACGCGATT
6.3% CpG methylation (1M)	ATAC m GCGTACTGCGGTTCGCGATCGCGCTCTCGC GCTGACGGTTCGTCGCGCGTACGCGATT
12.5% CpG methylation (2D)	ATAC m GCGTACTGCGGTTCGCGATCGCGCTCTCGC GCTGACGGTTCGTCGCGCGTACG m GATT
12.5% CpG methylation (2C)	ATACGCGTACTGCGGTTCGCGATCGCGCTCT m GC m GCTGACGGTTCGTCGCGCGTACGCGATT
12.5% CpG methylation (2E)	ATAC m G m GTA m CTACTGCGGTTCGCGATCGCGCTCTCG CGCTGACGGTTCGTCGCGCGTACGCGATT
25% CpG methylation (4D)	ATAC m GCGTACTGCGGTTCGCGAT m GCGCTCTCG CGCTGACGGT m GTCGCGCGTACG m GATT
25% CpG methylation (4C)	ATACGCGTACTGCGGTTCGCGAT m G m GCTCT m m G m GCTGACGGTTCGTCGCGCGTACGCGATT
25% CpG methylation (4E)	ATACGCGTACTGCGGTTCGCGATCGCGCTCTCGCGC TGACGGTTCGTCG m G m GTA m G m GATT
25% CpG methylation (4LR)	ATAC m G m GTA m CTACTGCGGTTCGCGATCGCGCTCTCG CGCTGACGGTTCGTCGCGCGTAC m G m GATT
25% CpG methylation (4M-80)	ATAC m GCGTACTGCGGTTCGCGAT m GCGCTCTCG CGCTGACGGTGATGGACTTGACTAAGGTTG m GT CGCGCGTACG m GATT
25% CpG methylation (4M-100)	ATAC m GCGTACTGCGGTTCGCGAT m GCGCTCTCG CGCTGACGGTGATGGACTTGACTAAGGTAGGTTA TGACAGGCTTAGAATG m GTTCGCGCGTACG m GA TT
50% CpG methylation (8M)	ATAC m GCGTACTG m GGT m GCGAT m GCGCTC TCG m GCTGACGGT m GTCGCG m GTACG m G ATT
100% CpG methylation (16M)	ATAC m G m GTA m CTACTG m GGT m G m GAT m G m G GCTCT m G m GCTGAC m GGT m G m GT m G m GC m GTAC m G m GATT
Unmethylated DNA (mixture experiment)	ATCTCGAACTTCTGACCTCAGGTGATCCTCCTGTC TTGGCCTCCCAAAGTGCTGCGATTAC
20CG	CGCGCGCGCGCGCGCGCGCG
20MCG	m G m G m G m G m G m G m G m G m G m G m G m G m G m G m G

Table S4 Comparison Table of microfluidic MeDIP-seq and our method

Feature	Microfluidic MeDIP-seq¹	Our Method
Target Material	Genomic DNA (~100–500 bp fragments)	Methylated oligonucleotide DNA (~60 bp fragments)
Sensitivity	0.5 ng DNA input	~1 ng/ μ L DNA input
Focus	Genome-wide methylation analysis	Targeted biomarker analysis
Applications	Cancer development studies, tissue-level epigenetics	Early disease diagnosis, liquid biopsy analysis
Output Complexity	High (genome-wide data)	Low (focused on actionable regions)

Reference:

1 Y. Zhu, Z. Cao, C. Lu, *Analyst*, 2019, **144**:1904–1915